Aplasia Ras homolog member I expression induces apoptosis in renal cancer cells via the β-catenin signaling pathway

JIAN YU, CHUI-ZE KONG, ZHE ZHANG, BO ZHAN and ZHEN-MING JIANG

Department of Urology, Institute of Urology, The First Affiliated Hospital of China Medical University, Shenyang, Liaoning 110001, P.R. China

Received January 21, 2014; Accepted September 18, 2014

DOI: 10.3892/mmr.2014.2742

Abstract. In numerous types of cancer, the Ras-associated tumor suppressor gene aplasia Ras homolog member I (*ARHI*), is downregulated. However, the function of ARHI in renal cancer remains to be elucidated. The present study investigated whether the suppressor gene *ARHI* influenced the growth of renal cancer cell lines and aimed to elucidate its mechanism of action, using the techniques of cell biology and molecular pathology. To the best of our knowledge, the present study was the first to determine the effects of ARHI on human renal cancer cells *in vivo* and *in vitro*. It was demonstrated that ARHI exhibited a tumor suppressor function in OS-RC-2 cells and acted via the β-catenin signaling pathway. It was additionally confirmed that the levels of ARHI messenger RNA and protein in renal cancer tissues were lower than those in matched normal tissues. These results provided a novel insight into the possible therapeutic applications of ARHI in renal cancer.

Introduction

Renal cell carcinoma (RCC) is a prevalent malignancy with ~64,000 novel cases diagnosed and 13,500 mortalities per year (1). Although major progression has been made in the therapeutic management of kidney cancer in the past decade, RCC remains the third most common type of urological cancer and is responsible for 3% of adult neoplasia (2).

Aplasia Ras homologue member I (*ARHI*) is a tumor suppressor gene localized to 1p31 which spans ~8 kb and contains two exons and one intron. *ARHI* encodes a 26-kDa guanosine triphosphatase (GTPase) with 55-62% homology to Ras and Rap, though its function may differ markedly from that of Ras and Rap (3,4). Downregulation of ARHI expression in breast, ovarian and stomach cancer may occur through loss of heterozygosity, DNA methylation or transcriptional regulation (5-8). Loss of ARHI expression is associated with tumor progression and poor prognosis (7,8). Evidence has suggested that overexpression of ARHI is able to inhibit cancer-cell growth in ovarian and breast cancers (9). However, the roles of ARHI in renal cancer remain to be elucidated.

In the present study, pathological and functional studies were performed in order to determine the role of ARHI in the suppression of renal cancer *in vivo* and *in vitro*. The expression levels of ARHI mRNA and protein in renal cancer were detected using polymerase chain reaction (PCR) and western-blot analyses. Further elucidation of the functions of ARHI may lead to an improved understanding of the pathogenesis of renal cancer and provide a novel therapeutic target.

Materials and methods

Patients. Surgical specimens of 52 renal cancers were obtained from the Department of Urology, Institute of Urology, The First Affiliated Hospital of China Medical University (Shenyang, China) between January 2008 and December 2012. None of the patients underwent radiotherapy or chemotherapy prior to operation. Patients gave their consent for the use of tumor tissues for clinical research and The First Affiliated Hospital of China Medical University Ethics Committee (Shenyang, China) approved the research protocols.

Cell lines. The human renal cancer cell line OS-RC-2 was purchased from the Shanghai Cell Bank of Type Culture Collection (Chinese Academy of Sciences, Shanghai, China) and maintained in RPMI-1640 medium (Gibco-BRL, Invitrogen Life Technologies, Carlsbad, CA, USA) containing 10% heat-inactivated fetal bovine serum (FBS; HyClone, GE Healthcare, Little Chalfont, UK), 100 U/ml penicillin G and 100 μg/ml streptomycin (Invitrogen, Carsbad, CA, USA) in a humidified 5% CO_2 incubator at 37˚C.

Transfection. The pcDNA3.1-ARHI vector (provided by Dr Jin Ji, China Medical University, Shenyang, China) was transfected into OS-RC-2 cells using Lipofectamine 2000 (Invitrogen Life Technologies, Carlsbad, CA, USA) according

Correspondence to: Dr Chui-Ze Kong, Department of Urology, Institute of Urology, The First Hospital of China Medical University, 155 Nanjing North Street, Shenyang, Liaoning 110001, P.R. China
E-mail: kongczcmu@163.com

Key words: aplasia Ras homolog member I, renal cell carcinoma, β-catenin, apoptosis, survival

to the manufacturer's instructions. Following 48 h of incubation at 37˚C, transfected cells were trypsinized and seeded into 60-mm dishes.

RNA isolation and reverse transcription quantitative (q) PCR. Total RNA was isolated from cells and tissues by using a TRIzol reagent (Invitrogen Life Technologies) according to the manufacturer's instructions. cDNA was synthesized from 2 μg total RNA. Oligo (dT) 16 and SuperScript II reverse transcriptase (Invitrogen Life Technologies) were used for the reverse transcription reaction, which was performed according to the manufacturer's instructions. The *ARHI* primers were as follows: forward, 5'-CAGCTGGTTTCTTACCACGTAT-3' and reverse, 5'-GCACAAGTTCTCCCACACTTAG-3'. To further quantify *ARHI* gene expression levels in renal cancer cells, the relative *ARHI* mRNA expression levels were measured by qPCR. A housekeeping gene, GAPDH was used as an endogenous control. The GAPDH primers were as follows: forward, 5'-AGAAGGCTGGGGCTCATTTG-3' and reverse, 5'-AGGGGCCATCCACAGTCTTC-3'. Relative quantification was calculated using the ΔΔCt method.

Immunofluorescence. Transfected cells were washed with phosphate-buffered saline (PBS), fixed in 4% paraformaldehyde, permeabilized in 1% Triton X-100 for 5 min and blocked with 5% bovine serum albumin in PBS containing 0.5% Triton X-100 for 1 h (Beyotime, Beijing, China). *ARHI* expression was detected using goat polyclonal immunoglobulin G (IgG) anti-ARHI antibody, dilution 1:100, (sc-30321, Santa Cruz Biotechnology, Inc., Dallas, TX, USA) for 1 h at room temperature. Cells were subsequently washed with PBS and incubated with Alexa Fluor® 594 donkey anti-goat IgG (heavy and light) (A11058, dilution 1:100; Invitrogen Life Technologies) for 1 h at room temperature, washed with PBS and mounted using SlowFade® Gold Antifade reagent (S36936; Invitrogen Life Technologies).

MTT assay. The proliferation rates of *ARHI*-transfected and control cells were measured by MTT assay. *ARHI*-transfected cells or control cells were plated at a density of $1x10^3$/well in 96-well plates and incubated for 48 h in complete culture medium containing 0.5 mg/ml MTT (Sigma-Aldrich, St. Louis, MO, USA). Following four hours of incubation, the medium was replaced with 100 μl dimethylsulfoxide (Sigma-Aldrich) and agitated for 10 min to dissolve the crystals. Absorbance optical density of each well was determined at 490 nm wavelength, including the subtraction of baseline reading (Bio-Rad, Hercules, CA, USA).

Cell cycle and apoptosis analysis. Cells ($3x10^5$/well) were plated and incubated overnight. Cells were trypsinized, collected in PBS and fixed on ice with 1% paraformaldehyde, followed by 70% cold ethanol. Following treatment with 10 μg/ml RNase (Beyotime), cells were stained with 50 μg/ml propidium iodide (PI; Sigma-Aldrich) for 15 min at room temperature for cell cycle analysis. Apoptotic cells were detected using Annexin V-fluorescein isothiocyanate (FITC)/PI double staining. The cells were trypsinized and stained with Annexin V-FITC and PI (KenGen, Nanjing, China). The stained cells were immediately analyzed using a FACSCalibur machine (BD Biosciences, Franklin Lakes, NJ, USA).

Xenograft assays. All experiments with animals were performed according to the guidelines of the China Medical University Ethical Committee. NU/NU Nude mice that were six to eight weeks-old were purchased from Vital River (Beijing, China). The mice were kept at a 12-h light/dark cycle (6:30 a.m. to 6:30 p.m.) at 22ºC with free access tofood and water. OS-RC-2 cells ($2x10^7$ in 200 μl) were subcutaneously injected into the axilla of each mouse. Once the tumor diameters reached 3-5 mm, the mice were divided randomly into three groups (untreated, mock or transfection) and received a 100 μl intratumoral injection of PBS, pCDNA3.1 or pCDNA3.1-ARHI, respectively. Three injections were administered at 9am, 3pm and 9pm every three days. Tumor growth was subsequently monitored for 30 days. Every five days until the end of the experiment, one mouse from each group was randomly selected to be anesthetized, photographed (Olympus CX31, Olympus, Tokyo, Japan) and sacrificed using spinal dislocation method. For each tumor, measurements were taken using calipers and tumor volumes were calculated as follows: length x $width^2$x0.52. Survival was monitored until the experiments were terminated due to heavy tumor burden.

Preparation of nuclear and cytoplasmic protein extracts. Nuclear and cytoplasmic protein fractions were isolated from cell lines at the time-points indicated in the manufacturer's instructions with the CelLytic™ NuCLEAR™ Extraction kit (Sigma-Aldrich). Protein concentrations were determined by bicinchoninic acid protein assay using bovine serum albumin as a standard (Pierce Biotechnology, Inc., Rockford, IL, USA).

Western blot analysis. Protein from cells and tissues (30 μg) was denatured in 6X loading buffer at 95°C for 5 min, separated by SDS-PAGE and transferred onto a nitrocellulose membrane (Beyotime). The membranes were subsequently incubated in 5% milk for 2 h at room temperature and then incubated with the primary antibody overnight at 4˚C. Primary antibodies included: goat polyclonal immunoglobulin G anti-ARHI (sc-30321, Santa Cruz Biotechnology, Inc.), rabbit polyclonal immunoglobulin G anti-low-density lipoprotein receptor-related protein 6 (LRP6) (sc-15399, Santa Cruz Biotechnology, Inc.), mouse polyclonal immunoglobulin G anti-phosphorylated-LRP6 (Ser1490) (#2568, Cell Signaling Technology, Beverly, MA, USA), rabbit monoclonal immunoglobulin G anti-Axin2 (#5863, Cell Signaling Technology), mouse monoclonal immunoglobulin G anti-glycogen synthase kinase 3β (GSK-3β; sc-81462, Santa Cruz Biotechnology, Inc.), mouse monoclonal immunoglobulin G anti-β-catenin (#610154, BD Biosciences), and mouse monoclonal immunoglobulin G anti-β-tubulin (T5201, Sigma-Aldrich). The following day, membranes were washed three times with PBS and subsequently incubated with the secondary antibody for 2 h at room temperature. The signals were detected using an enhanced chemiluminescence kit (GE Healthcare).

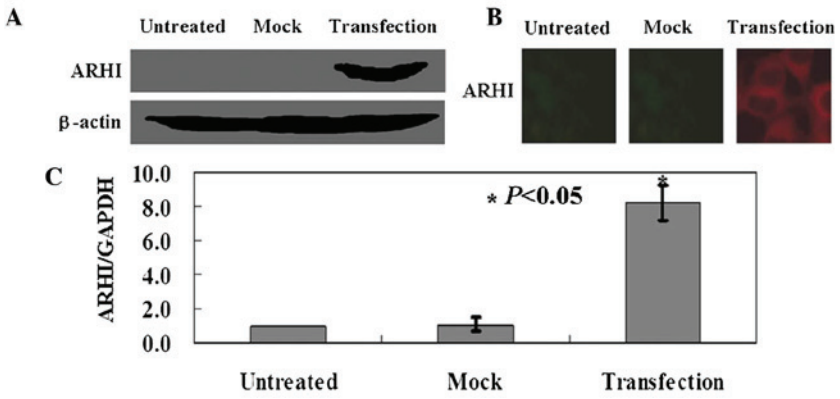

Figure 1. Detection of ARHI following transfection. (A) Detection of ARHI by western blotting. β-actin was used as an internal control. (B) Immunofluorescent detection of ARHI in transfected and untransfected OS-RC-2 cells (magnification, x200). (C) *ARHI* messenger RNA expression levels in OS-RC-2 cells and transfected OS-RC-2 cells detected using quantitative polymerase chain reaction. GAPDH was used as an internal control. Untreated, untreated OS-RC-2 cells; mock, OS-RC-2 cells transfected with pcDNA3.1; transfection, OS-RC-2 cells transfected with pcDNA3.1-ARHI. ARH1, aplasia Ras homologue member I.

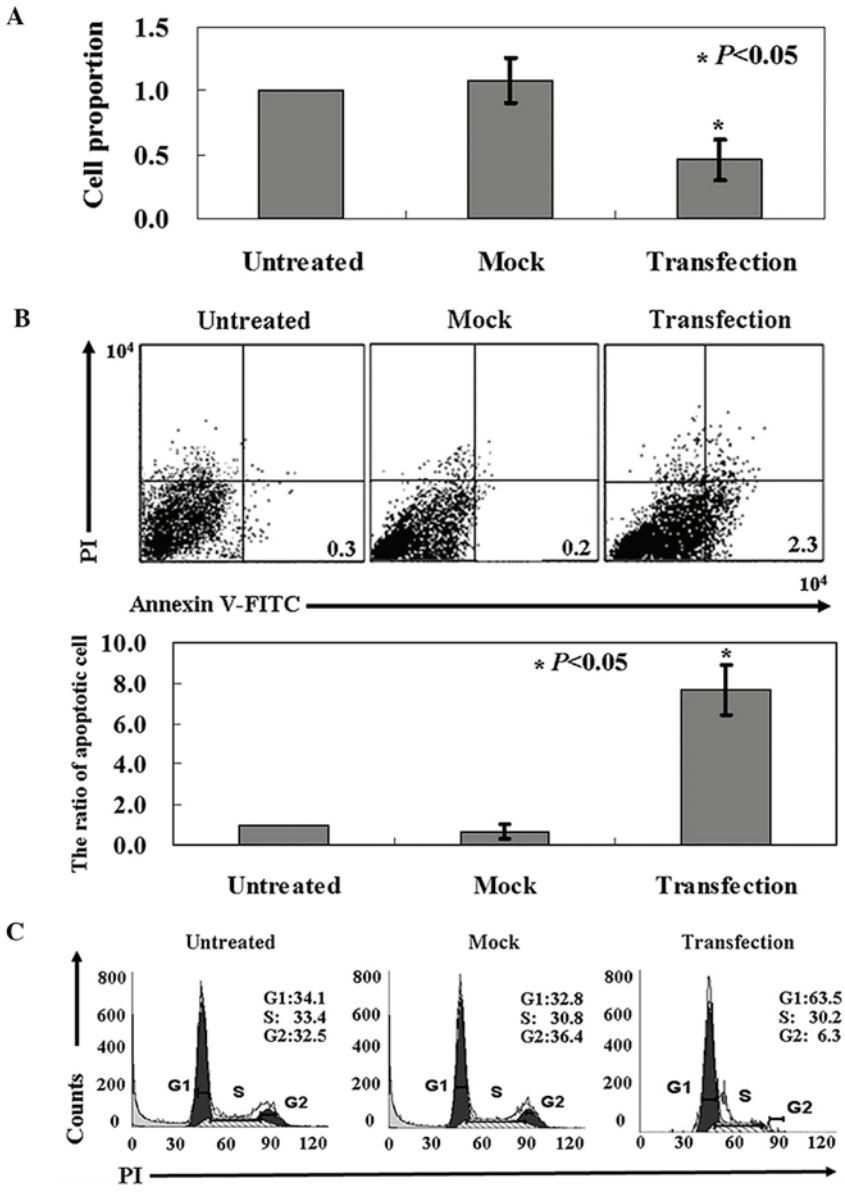

Figure 2. Anti-tumor activities of ARHI in OS-RC-2 cells. (A) The rate of growth inhibition of ARHI on cells was measured using MTT assay. (B) Apoptotic ratio of transfected and untransfected OS-RC-2 cells was analyzed by double staining with Annexin-V/PI. (C) PI staining indicated alterations in cell cycle progression. ARH1, aplasia Ras homologue member I; PI, propidium iodide; FITC, fluorescein isothiocyanate. Untreated, untreated OS-RC-2 cells; mock, OS-RC-2 cells transfected with pcDNA3.1; transfection, OS-RC-2 cells transfected with pcDNA3.1-ARHI.

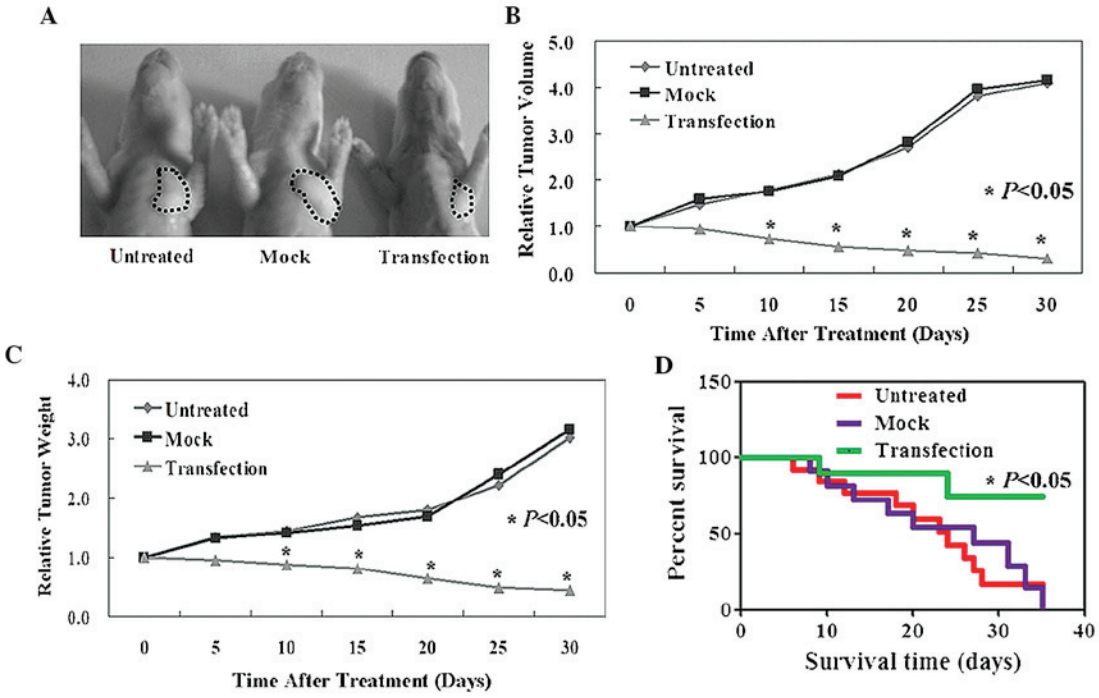

Figure 3. ARHI suppresses tumor growth in xenograft mouse models. (A) Gross appearance of subcutaneous tumors of xenograft mouse models in the untreated, mock and transfection groups. (B and D) Tumor volume and tumor weights of the three groups that were sacrificed 30 days following treatment. (C) Kaplan-Meier survival curves of the three groups. Untreated, untreated OS-RC-2 cells; mock, OS-RC-2 cells transfected with pcDNA3.1; transfection, OS-RC-2 cells transfected with pcDNA3.1-ARHI. ARH1, aplasia Ras homologue member I.

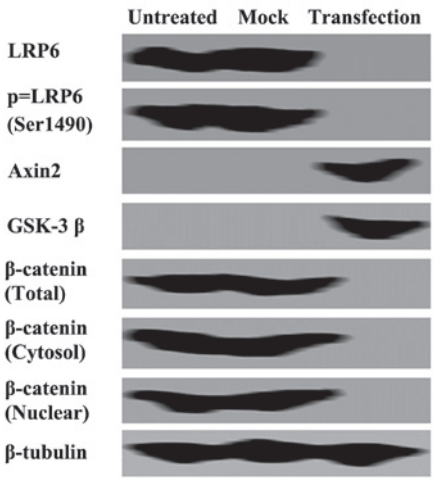

Figure 4. ARHI exhibits anti-tumor activity by blocking β-catenin signaling. Levels of Axin2, GSK-3β and total and phosphorylated forms of LRP6 were detected by western blot analysis of cell lysates. Total β-catenin, cytoplasmic β-catenin and nuclear β-catenin levels were also detected. β-tubulin was used as an internal control. Untreated, untreated OS-RC-2 cells; mock, OS-RC-2 cells transfected with pcDNA3.1; transfection, OS-RC-2 cells transfected with pcDNA3.1-ARHI. ARH1, aplasia Ras homologue member I; GSK-3β, glycogen synthase kinase-3β; LRP6, low-density lipoprotein receptor-related protein 6.

Immunohistochemical (IHC) staining. Immunohistochemistry was used to detect the expression of ARHI protein in renal cancer tissue samples. Immunohistochemical staining was performed on 4-μm sections obtained from formalin-fixed, paraffin-embedded blocks. Endogenous peroxidase activity was inhibited with 3% hydrogen peroxide for 30 min. Antigen retrieval was carried out in citrate buffer (10 mM, pH 6.0) for 30 min at 95˚C in a pressure cooker (Beyotime). The polyclonal antibody used was anti-*ARHI* (1:500; Santa Cruz Biotechnology, Inc.), which was applied and incubated overnight at 4˚C. Subsequently, sections were incubated with a biotinylated secondary antibody and then exposed to a streptavidin complex (horseradish peroxidase). Positive reactions were visualized with 3,3'-diaminobenzidine tetrahydrochloride (Sigma-Aldrich), followed by counterstaining with hematoxylin. Normal tissue was used as a positive control. Sections treated without primary antibodies were used as negative controls. The positive percentage of counted cells was graded semi-quantitatively according to a four-tier scoring system: Negative (-), 0-5%; weakly positive (+), 6-25%; moderately positive (++), 26-50%; and strongly positive (+++), 51-100%.

Statistical analysis. Values are expressed as the mean ± standard deviation of three independent experiments, each performed in triplicate with GraphPad Prism 5 (GraphPad Software, La Jolla, CA, USA). Kaplan-Meier survival plots were generated and comparisons between survival curves were made with the log-rank statistic. Differences between groups were assessed by unpaired, two-tailed Student's t-test. $P<0.05$ was considered to indicate a significant difference between values.

Results

ARHI is exogenously expressed in transfected OS-RC-2 cells. OS-RC-2 cells were transfected with the pcDNA3.1-*ARHI*

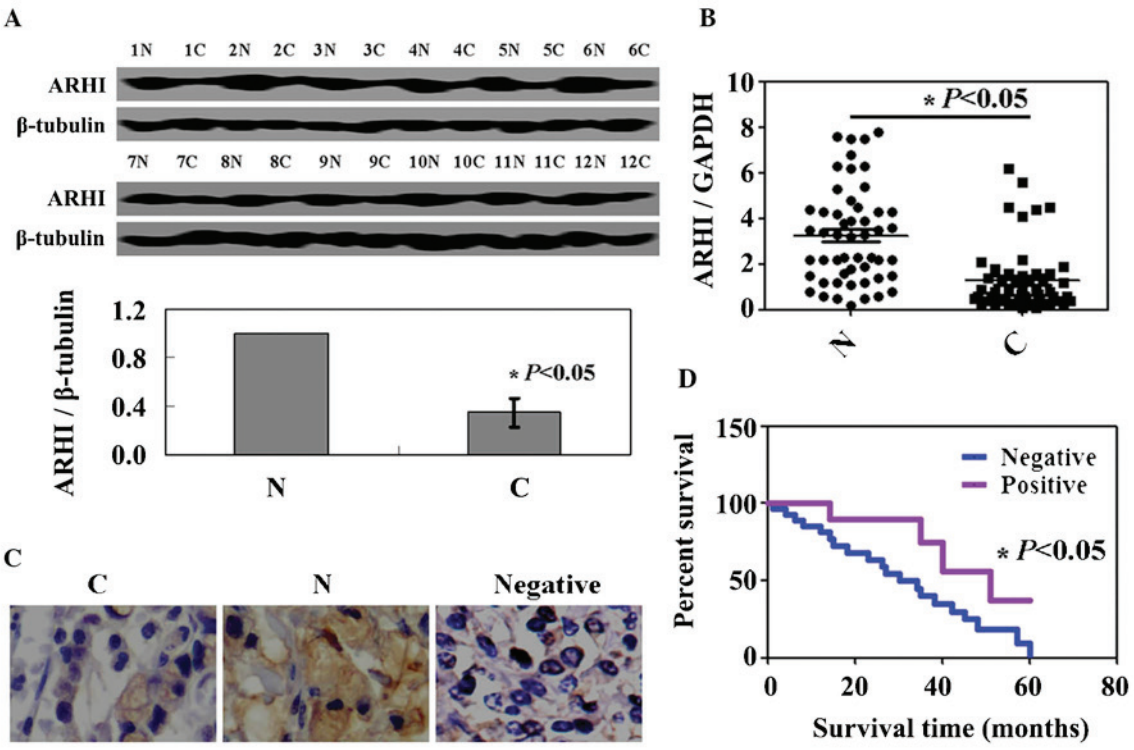

Figure 5. *ARHI* mRNA and protein expression levels in renal cancer tissues. (A) ARHI protein expression levels were measured by western blot analysis. β-tubulin was used as an internal control. (B) Polymerase chain reaction analysis of *ARHI* was performed in renal cancer tissues and adjacent noncancerous tissues. *GAPDH* was used as an internal control. (C) Representative images of renal cancer and corresponding noncancerous tissue with immunohistochemical staining using anti-ARHI antibody (magnification, x100). (D) Kaplan-Meier curves for cumulative survival rates of patients with renal cancer according to ARHI expression. N, normal tissue; C, cancer tissue; ARHI, aplasia Ras homologue member I.

expression vector, and the expression levels of *ARHI* protein and mRNA were measured by western blot analysis (Fig. 1A), immunofluorescence assay (Fig. 1B) and qPCR (Fig. 1C). As indicated in Fig. 1, the results confirmed exogenous expression of *ARHI* in OS-RC-2 cells following transfection.

Anti-tumor activity of ARHI in OS-RC-2 cells. MTT assay indicated a significantly lower growth rate in the ARHI-expressing OS-RC-2 cells than that in the untreated cells ($P<0.05$; Fig. 2A). Annexin-V/PI double staining demonstrated a higher level of apoptosis in ARHI-expressing OS-RC-2 cells vs mock cells or untransfected cells ($P<0.05$; Fig. 2B). PI staining of cells revealed that ARHI-expressing OS-RC-2 cells were arrested in the G_1 phase (Fig. 2C).

ARHI inhibits tumor growth and promotes survival rate in vivo. Established xenograft tumor models were used to determine whether ARHI exhibits antitumor properties *in vivo*. As indicated in Fig. 3A and B, the tumor volumes in ARHI-treated mice were significantly reduced in comparison to those of the PBS- or pCDNA-3.1-treated mice ($P<0.05$). Similarly, tumor weights in the ARHI-treated group were also significantly reduced compared to those of the PBS- and pCDNA-3.1-treated groups ($P<0.05$; Fig. 3C). It was additionally revealed that ARHI-treated mice displayed an improved survival rate in comparison with that of the PBS- and mock-treated mice ($P<0.05$; Fig. 3D).

ARHI blocks the β-catenin signaling pathway in OS-RC-2 cells. To examine the mechanisms induced by ARHI in OS-RC-2 cells, western blot analysis was performed. Cytoplasmic and nuclear β-catenin expression levels were significantly reduced following transfection with ARHI compared with those of the controls (Fig. 4). To determine the mechanism responsible for the decrease in β-catenin expression levels, the expression levels of LRP6 were examined. Western blot analysis detected a significant inhibition of LRP6 expression and phosphorylation following transfection with ARHI (Fig. 4). An increase in Axin2 and GSK-3β expression levels were also detected in ARHI-expressing cells compared with those of the controls (Fig. 4).

ARHI expression is reduced in renal cancer. ARHI expression in renal cancer specimens from 52 patients was decreased compared with those in matched normal tissues (Fig. 5A). As shown in Fig. 5B, the levels of *ARHI* mRNA expression in renal cancer specimens were lower than those in normal tissues. ARHI protein and mRNA expression levels were coincident. Immunostaining for ARHI was only localized in the cytoplasm. ARHI protein was markedly expressed in non-tumor parts of specimens (Fig. 5C). The association between the expression levels of ARHI and the clinicopathological characteristics of these patients is summarized in Table I. No correlation was found between gender, age, differentiation, histological grade, lymph node metastasis and tumor size ($P>0.05$). However, ARHI expression was significantly associated with T stage and distant metastasis ($P<0.05$). The cumulative survival rate of patients with ARHI expression was higher than that in those without ARHI expression ($P<0.05$; Fig. 5D).

Table I. Association between ARHI expression and the clinicopathological parameters of renal cancer.

		ARHI expression						
Clinicopathological feature	n	-	+	++	+++	PR (%)	χ^2	P
Gender							0.219	0.975
Female	18	15	1	1	1	16.7		
Male	34	29	2	2	1	14.7		
Age (years)							2.873	0.412
<65	15	11	1	2	1	26.7		
≥65	37	33	2	1	1	10.8		
Differentiation							0.912	0.823
Differentiated	22	18	1	2	1	18.2		
Undifferentiated	30	26	2	1	1	13.3		
Histological grade							4.597	0.204
I-II	32	29	2	1	0	9.3		
III-IV	20	15	1	2	2	25.0		
T stage							9.683	0.022
T1-T2	38	35	2	0	1	7.9		
T3-T4	14	9	1	3	1	35.7		
Lymph node metastasis							4.041	0.257
-	35	29	1	3	2	17.1		
+	17	15	2	0	0	11.8		
Tumor size							4.762	0.190
< 4 cm	11	8	2	1	0	27.3		
≥ 4 cm	41	36	1	2	2	12.2		
Distant metastasis							9.117	0.028
Absent	15	11	0	2	2	26.7		
Present	37	33	3	1	0	10.8		

PR, positive rate; ARHI, aplasia Ras homologue member I.

Discussion

ARHI has been demonstrated to act as a suppressor in numerous types of cancer (3,9,10). Previous studies have additionally indicated that ARHI inhibited cell proliferation and promoted apoptosis (9,11,10). Consistent with previous studies, the results of the present study confirmed the anti-tumor activity of ARHI in renal cancer cells. Additionally, ARHI inhibited tumor growth *in vivo*. To the best of our knowledge, the present study was the first to demonstrate the association between ARHI and renal cancer.

Numerous studies have demonstrated the mechanism of ARHI in cancer cells. ARHI inhibits the Ras/mitogen activated protein pathway, induces p21 (WAF1/CIP1) and downregulates cyclin D1 in cancer cells (3,5). A study revealed that ARHI regulates autophagy in ovarian cancer cells and leads to autophagic mortality in cell culture through inhibition of the mammalian target of rapamycin pathway (12). The results of the present study indicated that ARHI induced apoptosis via the β-catenin signaling pathway. In order to verify this molecular mechanism, all associated proteins in the β-catenin signaling pathway were detected. LRP6 is a Wnt co-receptor which functions in the Wnt/β-catenin signaling pathway, and its phosphorylation is required for the activation of Wnt/β-catenin signaling (13). LRP6 phosphorylation is followed by the formation of the axin-GSK-3β complex (14). In the absence of Wnt signaling, GSK-3β has been shown to be active (15), which leads to the degradation of cytoplasmic β-catenin and an inhibition of nuclear translocation (16). Cytoplasmic and nuclear β-catenin localization is considered an indicator of activated Wnt signaling (17,18). In the present study, the expression levels of GSK-3β and axin, as well as cytoplasmic and nuclear β-catenin expression levels detected in ARHI-expressing OS-RC-2 cells were consistent with the results of previous studies and confirmed that ARHI had the capacity to inhibit the proliferation of OS-RC-2 cells by suppression of the β-catenin signaling pathway.

In conclusion, to the best of our knowledge, the present study was the first to determine the effects of ARHI on human renal cancer cells *in vivo* and *in vitro*. The results demonstrated that ARHI had a tumor suppressor role in OS-RC-2 cells, exerting its effects via the β-catenin signaling pathway. These results provide a novel insight into the possible therapeutic applications of ARHI in renal cancer.

References

1. Siegel R, DeSantis C, Virgo K, Stein K, Mariotto A, Smith T, Cooper D, Gansler T, Lerro C, Fedewa S, *et al*: Cancer treatment and survivorship statistics, 2012. CA Cancer J Clin 62: 220-241, 2012.
2. Kelley JR and Duggan JM: Gastric cancer epidemiology and risk factors. J Clin Epidemiol 56: 1-9, 2003.
3. Luo RZ, Fang X, Marquez R, Liu SY, Mills GB, Liao WS, Yu Y and Bast RC: ARHI is a Ras-related small G-protein with a novel N-terminal extension that inhibits growth of ovarian and breast cancers. Oncogene 22: 2897-2909, 2003.
4. Hisatomi H, Nagao K, Wakita K and Kohno N: *ARHI*/NOEY2 inactivation may be important in breast cancer pathogenesis. Oncology 62: 136-140, 2002.
5. Yu Y, Xu F, Peng H, Fang X, Zhao S, Li Y, Cuevas B, Kuo WL, Gray JW, Siciliano M, *et al*: NOEY2 (ARHI), an imprinted putative tumor suppressor gene in ovarian and breast carcinomas. Proc Natl Acad Sci USA 96: 214-219, 1999.
6. Wang W, Bu XM, Wang J, Zhang N and Zhao CH: The expression of ARHI in pT2a and pT2b stage gastric cancer and its clinical significance. Oncol Rep 27: 1953-1959, 2012.
7. Rosen DG, Wang L, Jain AN, Lu KH, Luo RZ, Yu Y, Liu J and Bast RC Jr: Expression of the tumor suppressor gene ARHI in epithelial ovarian cancer is associated with increased expression of p21 WAF1/CIP1 and prolonged progression-free survival. Clin Cancer Res 10: 6559-6566, 2004.
8. Wang L, Hoque A, Luo RZ, Yuan J, Lu Z, Nishimoto A, Liu J, Sahin AA, Lippman SM, Bast RC Jr and Yu Y: Loss of the expression of the tumor suppressor gene ARHI is associated with progression of breast cancer. Clin Cancer Res 9 (10 Pt 1): 3660-3666, 2003.
9. Bao JJ, Le XF, Wang RY, Yuan J, Wang L, Atkinson EN, LaPushin R, Andreeff M, Fang B, Yu Y and Bast RC Jr: Reexpression of the tumor suppressor gene ARHI induces apoptosis in ovarian and breast cancer cells through a caspase-independent calpain-dependent pathway. Cancer Res 62: 7264-7272, 2002.
10. Tang HL, Hu YQ, Qin XP, Jazag A, Yang H, Yang YX, Yang XN, Liu JJ, Chen JM, Guleng B and Ren JL: Aplasia ras homolog member I is downregulated in gastric cancer and silencing its expression promotes cell growth in vitro. J Gastroenterol Hepatol 27: 1395-1404, 2012.
11. Huang S, Chang IS, Lin W, Ye W, Luo RZ, Lu Z, Lu Y, Zhang K, Liao WS, Tao T, Bast RC Jr, *et al*: ARHI (DIRAS3), an imprinted tumour suppressor gene, binds to importins and blocks nuclear import of cargo proteins. Biosci Rep 30: 159-168, 2009.
12. Lu Z, Luo RZ, Lu Y, Zhang X, Yu Q, Khare S, Kondo S, Kondo Y, Yu Y, Mills GB, *et al*: The tumor suppressor gene ARHI regulates autophagy and tumor dormancy in human ovarian cancer cells. J Clin Invest 118: 3917-3929, 2008.
13. Zeng X, Huang H, Tamai K, Zhang X, Harada Y, Yokota C, Almeida K, Wang J, Doble B, Woodgett J, *et al*: Initiation of wnt signaling: control of Wnt coreceptor Lrp6 phosphorylation/activation via frizzled, dishevelled and axin functions. Development 135: 367-375, 2008.
14. Bache KG, Slagsvold T and Stenmark H: Defective down-regulation of receptor tyrosine kinases in cancer. EMBO J 23: 2707-2712, 2004.
15. Ikeda S, Kishida S, Yamamoto H, Murai H, Koyama S and Kikuchi A: Axin, a negative regulator of the Wnt signaling pathway, forms a complex with GSK-3beta and beta-catenin and promotes GSK-3beta-dependent phosphorylation of beta-catenin. EMBO J 17: 1371-1384, 1998.
16. Aberle H, Bauer A, Stappert J, Kispert A and Kemler R: beta-catenin is a target for the ubiquitin-proteosome pathway. EMBO J 16: 3797-3804, 1997.
17. Anderson CB, Neufeld KL and White RL: Subcellular distribution of Wnt pathway proteins in normal and neoplastic colon. Proc Natl Acad Sci USA 99: 8683-8688, 2002.
18. Jin Z, Han YX and Han XR: Degraded iota-carrageenan can induce apoptosis in human osteosarcoma cells via the Wnt/β-catenin signaling pathway. Nutr Cancer 65: 126-131, 2013.